Design and Stabilization of Sampled-Data Neural-Network-Based Control Systems[1]

H.K. Lam and F.H.F. Leung
Centre for Multimedia Signal Processing, Department of Electronic and Information Engineering, The Hong Kong Polytechnic University, Hung Hom, Kowloon, Hong Kong

Abstract - This paper presents the design and stability analysis of sampled-data neural-network-based control systems. A continuous-time nonlinear plant and a sampled-data three-layer fully-connected feed-forward neural-network-based controller are connected in a closed-loop to perform a control task. Stability conditions will be derived to guarantee the closed-loop system stability. Linear-matrix-inequality- and genetic-algorithm-based approaches will be employed to obtain the maximum sampling period and connection weights of the neural network subject to the considerations of the system stability and performance. An application example will be given to illustrate the design procedure and effectiveness of the proposed approach.

1. INTRODUCTION

The superior learning and generalization abilities of neural networks have attracted the public attention for many years. It was shown that a three-layer fully-connected feed-forward neural-network (TLFCFFNN) is a universal approximator which is able to approximate any smooth continuous function in a compact domain to an arbitrary accuracy [1]. Because of this outstanding property, neural networks were widely applied in different applications to handle different problems such as forecasting, handwritten character recognitions, control problems, etc.

This paper focuses on the system stability and performance issues of the neural-network-based sampled-data control problems. A neural-network-based control system is composed of a nonlinear plant and a neural-network-based controller connected in closed-loop. The nonlinearities of the plant and neural network, and the complexity of the network structure make the analysis work difficult and complex. Different neural-network-based control approaches subject to the consideration of the system stability were proposed. In [2], an adaptive neural-network based controller with variable hidden nodes was presented. The stability of the closed-loop system is achieved through on-line parameter adaptation, which is governed by adaptive laws derived based on the Lyapunov stability theory. The main idea of this approach is to compensate the nonlinearity of the plant by making use of the on-line estimated parameter values. The estimation error is a potential component to cause the instability of the closed-loop system. To handle the effect of the estimation error to the system stability, adaptive neural-network based controllers [3]-[6] with switching control signals were proposed. These switching signals may introduce a chattering effect to the system. In [7]-[8], adaptive neural networks combined with other conventional controllers were proposed. In most of these approaches, the use of the neural networks is mainly for modeling the unknown nonlinearity of the plants. Another control schemes were then employed to achieve the system stability by compensating the system nonlinearity based on the learnt information of the neural networks. In summary, the system stability was achieved by adaptive and/or sliding mode control techniques in most of these approaches but not by the neural network itself. These approaches require that the network parameters are on-line changing according to some adaptive laws. This requirement will increase the computational demand, structural complexity, and implementation cost of the neural-network-based controller. In [9]-[11], stability conditions have been derived for a class of neural-network-based control systems with a feed-forward multilayer-perceptron (MLP) neural network. The derived stability conditions were only for checking the stability of the neural-network-based control systems. However, the ways for finding the network parameters and optimizing the system performance were ignored. These are in fact two important issues for putting the neural-network-based controller into practice.

In most of the published work, the efforts were put to purely continuous-time or discrete-time neural-network-based control systems. The sampled-data neural-network-based control systems are seldom considered. Fig. 1 shows the sampled-data TLFCFFNN-based control system, which is formed by a continuous-time nonlinear plant and a sampled-data TLFCFFNN-based controller connected in closed-loop. Referring to this figure, the sampled-data TLFCFFNN-based controller is formed by a sampler, a discrete-time TLFCFFNN-based controller and a zero-order-hold (ZOH) unit. The sampler takes the system states every h seconds to the discrete-time TLFCFFNN-based controller for generating the control signals. The constant time period h is called the sampling period. The control signals generated by the discrete-time TLFCFFNN-based controller will be fed to the ZOH unit to give the control signals to the nonlinear plant to realize the control process. The control signals from the ZOH unit are held constant during the sampling period. It can be seen that the introduction of the sampler and ZOH unit make the dynamics of the closed-loop system more complex, which increases the difficulty of the system analysis.

[1] The work described in this paper was fully supported by a grant from The Hong Kong Polytechnic University (Project No. G-YX31).

0-7803-9048-2/05/$20.00 ©2005 IEEE

However, under this control framework, the development and implementation costs may be reduced as the sampled-data TLFCFFNN-based controller can be realized by a microcomputer or a digital computer. In this paper, stability conditions will be derived to guarantee the stability of the TLFCFFNN-based control systems using the Lyapunov approach. The derived stability conditions will be employed to aid the design of stable sampled-data TLFCFFNN-based controllers. The finding of the maximum sampling period and connection weights of the TLFCFFNN-based controllers, and the optimization of the system performance subject to the system stability are formulated as a generalized eigenvalue minimization problem (GEVP) [12] and genetic algorithm (GA) [13] minimization problem respectively. These problems can be solved numerically by convex programming techniques [12] and GA [13].

2. Nonlinear System and Neural-Network-Based Controller

A TLFCFFNN-based control system as shown in Fig. 1 consists of a continuous-time nonlinear system and a TLFCFFNN-based controller.

A. Nonlinear System

The continuous-time nonlinear system has the following form:

$$\dot{\mathbf{x}}(t) = \mathbf{f}\big(\mathbf{x}(t), \mathbf{u}(t)\big) \tag{1}$$

where $\mathbf{x}(t) = [x_1(t) \quad x_2(t) \quad \cdots \quad x_n(t)]^{\mathrm{T}}$ is the system state vector; $\mathbf{u}(t) = [u_1(t) \quad u_2(t) \quad \cdots \quad u_m(t)]^{\mathrm{T}}$ is the input vector; $\mathbf{f}(\cdot)$ denotes a nonlinear function with a known form. It is assumed that the nonlinear system of (1) can be written as,

$$\dot{\mathbf{x}}(t) = \sum_{i=1}^{p} w_i(\mathbf{x}(t))\big(\mathbf{A}_i\mathbf{x}(t) + \mathbf{B}_i\mathbf{u}(t)\big) \tag{2}$$

where $\mathbf{A}_i \in \Re^{n\times n}$ and $\mathbf{B}_i \in \Re^{n\times m}$ are the constant system and input matrices respectively; p is a nonzero positive integer; $w_i(\mathbf{x}(t))$ has the following properties:

$$\sum_{i=1}^{p} w_i(\mathbf{x}(t)) = 1, \quad w_i(\mathbf{x}(t)) \in [0 \quad 1], \; i = 1, 2, ..., p \tag{3}$$

It should be noted that the value of $w_i(\mathbf{x}(t))$ is unknown if the nonlinear system is subject to parameter uncertainties.

B. Sampled-Data Three-Layer Fully-Connected Feed-Forward Neural-Network-Based Controller

The input-output relationship of a discrete-time TLFCFFNN [14] is defined as,

$$y_k(t_\gamma) = \sum_{j=1}^{n_h} g_{k,j} t_f\left(\sum_{i=1}^{n} m_{j,i} x_i(t_\gamma) + b_j\right), \; k = 1, 2, \ldots, n_{out} \tag{4}$$

where $t_\gamma = \gamma h$, $\gamma = 0, 1, 2, ...$, denotes a sampled instance; $h = t_{\gamma+1} - t_\gamma$ denotes the constant sampling period; $m_{j,i}$ denotes the connection weight between the j-th hidden node and the i-th input node; $g_{k,j}$ denotes the connection weight between the k-th output node and the j-th hidden node; b_j denotes the bias for the j-th hidden node; $t_f(\cdot)$ denotes the activation function; n_{out} denotes the number of output nodes; $\mathbf{x}(t_\gamma) = [x_1(t_\gamma) \quad x_2(t_\gamma) \quad \cdots \quad x_n(t_\gamma)]^{\mathrm{T}}$ denotes the sampled system state vector $\mathbf{x}(t)$ at the sampled time t_γ. The sampled-data TLFCFFNN-based controller for the nonlinear system of (2), with $n_{out} = mn$, is defined as,

$$\mathbf{u}(t) = \frac{\begin{bmatrix} y_1(t_\gamma) & y_2(t_\gamma) & \cdots & y_n(t_\gamma) \\ y_{n+1}(t_\gamma) & y_{n+2}(t_\gamma) & \cdots & y_{2n}(t_\gamma) \\ \vdots & \vdots & \ddots & \vdots \\ y_{(m-1)n+1}(t_\gamma) & y_{(m-1)n+2}(t_\gamma) & \cdots & y_{mn}(t_\gamma) \end{bmatrix}\begin{bmatrix} x_1(t_\gamma) \\ x_2(t_\gamma) \\ \vdots \\ x_n(t_\gamma) \end{bmatrix}}{\sum_{l=1}^{n_h} t_f\left(\sum_{i=1}^{n} m_{l,i} x_i(t_\gamma) + b_l\right)}, \; t_\gamma < t \le t_{\gamma+1} \tag{5}$$

It should be noted that $\mathbf{u}(t) = \mathbf{u}(t_\gamma)$ holds a constant vector value by a ZOH unit for $t_\gamma < t \le t_{\gamma+1}$. From (4) and (5), we have,

$$\mathbf{u}(t) = \frac{\left(\sum_{j=1}^{n_h} t_f\left(\sum_{i=1}^{n} m_{j,i} x_i(t_\gamma) + b_j\right)\right)\begin{bmatrix} g_{1,j} & g_{2,j} & \cdots & g_{n,j} \\ g_{n+1,j} & g_{n+2,j} & \cdots & g_{2n,j} \\ \vdots & \vdots & \ddots & \vdots \\ g_{(m-1)n+1,j} & g_{(m-1)n+2,j} & \cdots & g_{mn,j} \end{bmatrix}\begin{bmatrix} x_1(t_\gamma) \\ x_2(t_\gamma) \\ \vdots \\ x_n(t_\gamma) \end{bmatrix}}{\sum_{l=1}^{n_h} t_f\left(\sum_{i=1}^{n} m_{l,i} x_i(t_\gamma) + b_l\right)}$$

$$= \sum_{j=1}^{n_h} m_j(\mathbf{x}(t))\mathbf{G}_j\mathbf{x}(t_\gamma) \tag{6}$$

where

$$\mathbf{G}_j = \begin{bmatrix} g_{1,j} & g_{2,j} & \cdots & g_{n,j} \\ g_{n+1,j} & g_{n+2,j} & \cdots & g_{2n,j} \\ \vdots & \vdots & \ddots & \vdots \\ g_{(m-1)n+1,j} & g_{(m-1)n+2,j} & \cdots & g_{mn,j} \end{bmatrix} \tag{7}$$

$$m_j(\mathbf{x}(t_\gamma)) = \frac{t_f\left(\sum_{i=1}^{n} m_{j,i} x_i(t_\gamma) + b_j\right)}{\sum_{l=1}^{n_h} t_f\left(\sum_{i=1}^{n} m_{l,i} x_i(t_\gamma) + b_l\right)} \in [0 \quad 1] \tag{8}$$

which has the property that $\sum_{j=1}^{n_h} m_j(\mathbf{x}(t_\gamma)) = 1$. It is assumed that the activation function $t_f(\cdot)$ is chosen such that $t_f\left(\sum_{i=1}^{n} m_{j,i} x_i(t_\gamma) + b_j\right) > 0$ and $\sum_{l=1}^{n_h} t_f\left(\sum_{i=1}^{n} m_{l,i} x_i(t_\gamma) + b_l\right) \neq 0$ at any time to satisfy the property of (8).

C. Sampled-Data TLFCFFNN-Based Control Systems

A sampled-data TLFCFFNN-based control system as shown in Fig. 1 is formed by connecting the continuous-time nonlinear system of (2) and the sampled-data TLFCFFNN-based controller of (6) in closed-loop. In the following, $w_i(\mathbf{x}(t))$ and $m_j(\mathbf{x}(t_\gamma))$ are written as w_i and m_j respectively. From (2) and (6), and with the property that $\sum_{i=1}^{p} w_i = \sum_{j=1}^{n_h} m_j = \sum_{i=1}^{p}\sum_{j=1}^{n_h} w_i m_j = 1$, we have,

$$\dot{\mathbf{x}}(t) = \sum_{i=1}^{p}\sum_{j=1}^{n_h} w_i m_j\big(\mathbf{A}_i\mathbf{x}(t) + \mathbf{B}_i\mathbf{G}_j\mathbf{x}(t_\gamma)\big) \tag{9}$$

Let $\tau(t) = t - t_\gamma \le h$ for $t_\gamma < t \le t_{\gamma+1}$. From (9), we have,

$$\dot{\mathbf{x}}(t)=\sum_{i=1}^{p}\sum_{j=1}^{n_h} w_i m_j\left(\mathbf{A}_i\mathbf{x}(t)+\mathbf{B}_i\mathbf{G}_j\mathbf{x}(t-\tau(t))\right) \tag{10}$$

III. Stability and Design of Sample-Data TLFCFFNN-Based Control Systems

The stability, design and performance optimization of the sampled-data TLFCFFNN-based control system of (10) will be investigated in this section.

A. Stability Analysis and Maximum Sampling Period

Consider the following Lyapunov function candidate to investigate the stability of the sampled-data TLFCFFNN-based control system,

$$V(t)=V_1(t)+V_2(t)+V_3(t) \tag{11}$$

where

$$V_1(t)=\mathbf{x}(t)^{\mathrm{T}}\mathbf{P}\mathbf{x}(t) \tag{12}$$

$$V_2(t)=\int_{-h}^{0}\int_{+\sigma}\dot{\mathbf{x}}(\varphi)^{\mathrm{T}}\mathbf{R}\dot{\mathbf{x}}(\varphi)d\varphi d\sigma \tag{13}$$

$$V_3(t)=\int_{-\tau(t)}^{}\mathbf{x}(\varphi)^{\mathrm{T}}\mathbf{S}\mathbf{x}(\varphi)d\varphi \tag{14}$$

where $\mathbf{P}$, $\mathbf{R}$ and $\mathbf{S}\in\Re^{n\times n}$ are symmetric positive definite matrices. From (10) and (12),

$$\begin{aligned}\dot{V}_1(t)&=\dot{\mathbf{x}}(t)^{\mathrm{T}}\mathbf{P}\mathbf{x}(t)+\mathbf{x}(t)^{\mathrm{T}}\mathbf{P}\dot{\mathbf{x}}(t)\\&\le\sum_{i=1}^{p}\sum_{j=1}^{n_h}w_i m_j\mathbf{x}(t)^{\mathrm{T}}\left(\mathbf{A}_i^{\mathrm{T}}\mathbf{P}+\mathbf{P}\mathbf{A}_i\right)\mathbf{x}(t)+\sum_{i=1}^{p}\sum_{j=1}^{n_h}w_i m_j\mathbf{x}(t-\tau(t))^{\mathrm{T}}\mathbf{G}_j^{\mathrm{T}}\mathbf{B}_i^{\mathrm{T}}\mathbf{P}\mathbf{x}(t)\\&\quad+\sum_{i=1}^{p}\sum_{j=1}^{n_h}w_i m_j\mathbf{x}(t)^{\mathrm{T}}\mathbf{P}\mathbf{B}_i\mathbf{G}_j\mathbf{x}(t-\tau(t))+\sum_{i=1}^{p}\sum_{j=1}^{n_h}w_i m_j\int_{-\tau(t)}\begin{bmatrix}\mathbf{x}(t)\\\dot{\mathbf{x}}(\varphi)\end{bmatrix}^{\mathrm{T}}\begin{bmatrix}\overline{\mathbf{R}}_{ij}&\hat{\mathbf{R}}_{ij}\\\hat{\mathbf{R}}_{ij}^{\mathrm{T}}&\mathbf{R}\end{bmatrix}\begin{bmatrix}\mathbf{x}(t)\\\dot{\mathbf{x}}(\varphi)\end{bmatrix}d\varphi\end{aligned} \tag{15}$$

where $\overline{\mathbf{R}}_{ij}\in\Re^{n\times n}$ is a symmetric positive definite matrix, $\hat{\mathbf{R}}_{ij}\in\Re^{n\times n}$ is an arbitrary matrix and $\begin{bmatrix}\overline{\mathbf{R}}_{ij}&\hat{\mathbf{R}}_{ij}\\\hat{\mathbf{R}}_{ij}^{\mathrm{T}}&\mathbf{R}\end{bmatrix}\ge 0$ for all i and j. From (15),

$$\begin{aligned}\dot{V}_1(t)&\le\sum_{i=1}^{p}\sum_{j=1}^{n_h}w_i m_j\mathbf{x}(t)^{\mathrm{T}}\left(\mathbf{A}_i^{\mathrm{T}}\mathbf{P}+\mathbf{P}\mathbf{A}_i\right)\mathbf{x}(t)+\sum_{i=1}^{p}\sum_{j=1}^{n_h}w_i m_j\mathbf{x}(t-\tau(t))^{\mathrm{T}}\mathbf{G}_j^{\mathrm{T}}\mathbf{B}_i^{\mathrm{T}}\mathbf{P}\mathbf{x}(t)\\&\quad+\sum_{i=1}^{p}\sum_{j=1}^{n_h}w_i m_j\mathbf{x}(t)^{\mathrm{T}}\mathbf{P}\mathbf{B}_i\mathbf{G}_j\mathbf{x}(t-\tau(t))+\sum_{i=1}^{p}\sum_{j=1}^{n_h}w_i m_j\tau(t)\mathbf{x}(t)^{\mathrm{T}}\overline{\mathbf{R}}_{ij}\mathbf{x}(t)\\&\quad+\sum_{i=1}^{p}\sum_{j=1}^{n_h}w_i m_j\int_{-\tau(t)}\dot{\mathbf{x}}(\varphi)^{\mathrm{T}}d\varphi\hat{\mathbf{R}}_{ij}^{\mathrm{T}}\mathbf{x}(t)+\sum_{i=1}^{p}\sum_{j=1}^{n_h}w_i m_j\mathbf{x}(t)^{\mathrm{T}}\hat{\mathbf{R}}_{ij}\int_{-\tau(t)}\dot{\mathbf{x}}(\varphi)d\varphi\\&\quad+\int_{-\tau(t)}\dot{\mathbf{x}}(\varphi)^{\mathrm{T}}\mathbf{R}\dot{\mathbf{x}}(\varphi)d\varphi\end{aligned} \tag{16}$$

Considering the fact that $\tau(t)\le h$ and the following relationship,

$$\int_{-\tau(t)}\dot{\mathbf{x}}(\varphi)d\varphi=\mathbf{x}(t)-\mathbf{x}(t-\tau(t)) \tag{17}$$

From (16) and (17), we have,

$$\begin{aligned}\dot{V}_1&=\sum_{i=1}^{p}\sum_{j=1}^{n_h}w_i m_j\begin{bmatrix}\mathbf{x}(t)\\\mathbf{x}(t-\tau(t))\end{bmatrix}^{\mathrm{T}}\begin{bmatrix}\mathbf{A}_i^{\mathrm{T}}\mathbf{P}+\mathbf{P}\mathbf{A}_i+h\overline{\mathbf{R}}_{ij}+\hat{\mathbf{R}}_{ij}+\hat{\mathbf{R}}_{ij}^{\mathrm{T}}&\mathbf{P}\mathbf{B}_i\mathbf{G}_j-\hat{\mathbf{R}}_{ij}\\\mathbf{G}_j^{\mathrm{T}}\mathbf{B}_i^{\mathrm{T}}\mathbf{P}-\hat{\mathbf{R}}_{ij}^{\mathrm{T}}&\mathbf{0}\end{bmatrix}\begin{bmatrix}\mathbf{x}(t)\\\mathbf{x}(t-\tau(t))\end{bmatrix}\\&\quad+\int_{-\tau(t)}\dot{\mathbf{x}}(\varphi)^{\mathrm{T}}\mathbf{R}\dot{\mathbf{x}}(\varphi)d\varphi\end{aligned} \tag{18}$$

From (10) and (13),

$$\begin{aligned}\dot{V}_2(t)&=h\dot{\mathbf{x}}(t)^{\mathrm{T}}\mathbf{R}\dot{\mathbf{x}}(t)-\int_{-h}\dot{\mathbf{x}}(\varphi)^{\mathrm{T}}\mathbf{R}\dot{\mathbf{x}}(\varphi)d\varphi\\&=h\left(\sum_{i=1}^{p}\sum_{j=1}^{n_h}w_i m_j\left[\mathbf{A}_i\quad\mathbf{B}_i\mathbf{G}_j\right]\begin{bmatrix}\mathbf{x}(t)\\\mathbf{x}(t-\tau(t))\end{bmatrix}\right)^{\mathrm{T}}\mathbf{R}\left(\sum_{k=1}^{p}\sum_{l=1}^{n_h}w_k m_l\left[\mathbf{A}_k\quad\mathbf{B}_k\mathbf{G}_l\right]\begin{bmatrix}\mathbf{x}(t)\\\mathbf{x}(t-\tau(t))\end{bmatrix}\right)\\&\quad-\int_{-h}\dot{\mathbf{x}}(\varphi)^{\mathrm{T}}\mathbf{R}\dot{\mathbf{x}}(\varphi)d\varphi\\&=h\sum_{i=1}^{p}\sum_{j=1}^{n_h}\sum_{k=1}^{p}\sum_{l=1}^{n_h}w_i m_j w_k m_l\begin{bmatrix}\mathbf{x}(t)\\\mathbf{x}(t-\tau(t))\end{bmatrix}^{\mathrm{T}}\begin{bmatrix}\mathbf{A}_i^{\mathrm{T}}\\\mathbf{G}_j^{\mathrm{T}}\mathbf{B}_i^{\mathrm{T}}\end{bmatrix}\mathbf{R}\left[\mathbf{A}_k\quad\mathbf{B}_k\mathbf{G}_l\right]\begin{bmatrix}\mathbf{x}(t)\\\mathbf{x}(t-\tau(t))\end{bmatrix}\\&\quad-\int_{-h}\dot{\mathbf{x}}(\varphi)^{\mathrm{T}}\mathbf{R}\dot{\mathbf{x}}(\varphi)d\varphi\end{aligned} \tag{19}$$

(19) can be further simplified by considering the following property:

$$\begin{aligned}&\sum_{i=1}^{p}\sum_{j=1}^{n_h}w_i m_j\begin{bmatrix}\mathbf{x}(t)\\\mathbf{x}(t-\tau(t))\end{bmatrix}^{\mathrm{T}}\begin{bmatrix}\mathbf{A}_i^{\mathrm{T}}\\\mathbf{G}_j^{\mathrm{T}}\mathbf{B}_i^{\mathrm{T}}\end{bmatrix}\mathbf{R}\left[\mathbf{A}_i\quad\mathbf{B}_i\mathbf{G}_j\right]\begin{bmatrix}\mathbf{x}(t)\\\mathbf{x}(t-\tau(t))\end{bmatrix}\\&\ge\sum_{i=1}^{p}\sum_{j=1}^{n_h}\sum_{k=1}^{p}\sum_{l=1}^{n_h}w_i m_j w_k m_l\begin{bmatrix}\mathbf{x}(t)\\\mathbf{x}(t-\tau(t))\end{bmatrix}^{\mathrm{T}}\begin{bmatrix}\mathbf{A}_i^{\mathrm{T}}\\\mathbf{G}_j^{\mathrm{T}}\mathbf{B}_i^{\mathrm{T}}\end{bmatrix}\mathbf{R}\left[\mathbf{A}_k\quad\mathbf{B}_k\mathbf{G}_l\right]\begin{bmatrix}\mathbf{x}(t)\\\mathbf{x}(t-\tau(t))\end{bmatrix}\end{aligned} \tag{20}$$

From (19) and (20), we have,

$$\begin{aligned}\dot{V}_2(t)&\le h\sum_{i=1}^{p}\sum_{j=1}^{n_h}w_i m_j\begin{bmatrix}\mathbf{x}(t)\\\mathbf{x}(t-\tau(t))\end{bmatrix}^{\mathrm{T}}\begin{bmatrix}\mathbf{A}_i^{\mathrm{T}}\mathbf{R}\mathbf{A}_i&\mathbf{A}_i^{\mathrm{T}}\mathbf{R}\mathbf{B}_i\mathbf{G}_j\\\mathbf{G}_j^{\mathrm{T}}\mathbf{B}_i^{\mathrm{T}}\mathbf{R}\mathbf{A}_i&\mathbf{G}_j^{\mathrm{T}}\mathbf{B}_i^{\mathrm{T}}\mathbf{R}\mathbf{B}_i\mathbf{G}_j\end{bmatrix}\begin{bmatrix}\mathbf{x}(t)\\\mathbf{x}(t-\tau(t))\end{bmatrix}\\&\quad-\int_{-h}\dot{\mathbf{x}}(\varphi)^{\mathrm{T}}\mathbf{R}\dot{\mathbf{x}}(\varphi)d\varphi\end{aligned} \tag{21}$$

From (14),

$$\begin{aligned}\dot{V}_3(t)&=\mathbf{x}(t)^{\mathrm{T}}\mathbf{S}\mathbf{x}(t)-\mathbf{x}(t-\tau(t))^{\mathrm{T}}\mathbf{S}\mathbf{x}(t-\tau(t))\\&=\begin{bmatrix}\mathbf{x}(t)\\\mathbf{x}(t-\tau(t))\end{bmatrix}^{\mathrm{T}}\begin{bmatrix}\mathbf{S}&\mathbf{0}\\\mathbf{0}&-\mathbf{S}\end{bmatrix}\begin{bmatrix}\mathbf{x}(t)\\\mathbf{x}(t-\tau(t))\end{bmatrix}\end{aligned} \tag{22}$$

From (11), (18), (21) to (22) and with the property that $\sum_{i=1}^{p}w_i=\sum_{j=1}^{n_h}m_j=\sum_{i=1}^{p}\sum_{j=1}^{n_h}w_i m_j=1$, we have,

$$\begin{aligned}\dot{V}(t)&\le\sum_{i=1}^{p}\sum_{j=1}^{n_h}w_i m_j\begin{bmatrix}\mathbf{x}(t)\\\mathbf{x}(t-\tau(t))\end{bmatrix}^{\mathrm{T}}\begin{bmatrix}\mathbf{Q}_{ij}^{(1,1)}&\mathbf{Q}_{ij}^{(1,2)}\\\mathbf{Q}_{ij}^{(1,2)^{\mathrm{T}}}&\mathbf{Q}_{ij}^{(2,2)}\end{bmatrix}\begin{bmatrix}\mathbf{x}(t)\\\mathbf{x}(t-\tau(t))\end{bmatrix}\\&\quad+\int_{-\tau(t)}\dot{\mathbf{x}}(\varphi)^{\mathrm{T}}\mathbf{R}\dot{\mathbf{x}}(\varphi)d\varphi-\int_{-h}\dot{\mathbf{x}}(\varphi)^{\mathrm{T}}\mathbf{R}\dot{\mathbf{x}}(\varphi)d\varphi\\&=\sum_{i=1}^{p}\sum_{j=1}^{n_h}w_i m_j\mathbf{z}(t)^{\mathrm{T}}\mathbf{Q}_{ij}\mathbf{z}(t)+\int_{-\tau(t)}\dot{\mathbf{x}}(\varphi)^{\mathrm{T}}\mathbf{R}\dot{\mathbf{x}}(\varphi)d\varphi-\int_{-h}\dot{\mathbf{x}}(\varphi)^{\mathrm{T}}\mathbf{R}\dot{\mathbf{x}}(\varphi)d\varphi\end{aligned} \tag{23}$$

where $\mathbf{z}(t)=\begin{bmatrix}\mathbf{x}(t)\\\mathbf{x}(t-\tau(t))\end{bmatrix}$,

$\mathbf{Q}_{ij}^{(1,1)}=\mathbf{A}_i^{\mathrm{T}}\mathbf{P}+\mathbf{P}\mathbf{A}_i+\hat{\mathbf{R}}_{ij}+\hat{\mathbf{R}}_{ij}^{\mathrm{T}}+\mathbf{S}+h\left(\overline{\mathbf{R}}_{ij}+\mathbf{A}_i^{\mathrm{T}}\mathbf{R}\mathbf{A}_i\right)$,

$\mathbf{Q}_{ij}^{(1,2)}=\mathbf{P}\mathbf{B}_i\mathbf{G}_j-\hat{\mathbf{R}}_{ij}+h\mathbf{A}_i^{\mathrm{T}}\mathbf{R}\mathbf{B}_i\mathbf{G}_j$,

$\mathbf{Q}_{ij}^{(2,2)}=h\mathbf{G}_j^{\mathrm{T}}\mathbf{B}_i^{\mathrm{T}}\mathbf{R}\mathbf{B}_i\mathbf{G}_j-\mathbf{S}$, $\mathbf{Q}_{ij}=\begin{bmatrix}\mathbf{Q}_{ij}^{(1,1)}&\mathbf{Q}_{ij}^{(1,2)}\\\mathbf{Q}_{ij}^{(1,2)^{\mathrm{T}}}&\mathbf{Q}_{ij}^{(2,2)}\end{bmatrix}$.

As $\tau(t)\le h$ and $\mathbf{R}>0$ which implies $\int_{-\tau(t)}\dot{\mathbf{x}}(\varphi)^{\mathrm{T}}\mathbf{R}\dot{\mathbf{x}}(\varphi)d\varphi-\int_{-h}\dot{\mathbf{x}}(\varphi)^{\mathrm{T}}\mathbf{R}\dot{\mathbf{x}}(\varphi)d\varphi\le 0$, we have,

$$\dot{V}(t)\le\sum_{i=1}^{p}\sum_{j=1}^{c}w_i m_j\mathbf{z}(t)^{\mathrm{T}}\mathbf{Q}_{ij}\mathbf{z}(t) \tag{24}$$

It can be seen from (24) that $\dot{V}(t) \le 0$ (equality holds when $\mathbf{z}(t) = 0$) if $\mathbf{Q}_{ij} < 0$ and $\begin{bmatrix} \overline{\mathbf{R}}_{ij} & \hat{\mathbf{R}}_{ij} \\ \hat{\mathbf{R}}_{ij}^{\mathrm{T}} & \mathbf{R} \end{bmatrix} \ge 0$ for all i and j. This implies that the sampled-data TLFCFFNN-based control system is asymptotically stable, e.g., $\mathbf{z}(t) \to 0$ as $t \to \infty \Rightarrow \mathbf{x}(t) \to 0$ as $t \to \infty$. By Schur complement [12], $\mathbf{Q}_{ij} < 0$ is equivalent to the following LMI,

$$\begin{bmatrix} \mathbf{A}_i^{\mathrm{T}}\mathbf{P} + \mathbf{P}\mathbf{A}_i + \hat{\mathbf{R}}_{ij} + \hat{\mathbf{R}}_{ij}^{\mathrm{T}} + \mathbf{S} + h\overline{\mathbf{R}}_{ij} & \mathbf{P}\mathbf{B}_i\mathbf{G}_j - \hat{\mathbf{R}}_{ij} & h\mathbf{A}_i^{\mathrm{T}}\mathbf{R} \\ \mathbf{G}_j^{\mathrm{T}}\mathbf{B}_i^{\mathrm{T}}\mathbf{P} - \hat{\mathbf{R}}_{ij}^{\mathrm{T}} & -\mathbf{S} & h\mathbf{G}_j^{\mathrm{T}}\mathbf{B}_i^{\mathrm{T}}\mathbf{R} \\ h\mathbf{R}\mathbf{A}_i & h\mathbf{R}\mathbf{B}_i\mathbf{G}_j & -h\mathbf{R} \end{bmatrix} < 0$$

Pre-multiply and post-multiply $\mathrm{diag}\{\mathbf{P}^{-1}, \mathbf{P}^{-1}, \mathbf{R}^{-1}\}$ to the above equation and let $\mathbf{X} = \mathbf{P}^{-1}$, $\hat{\mathbf{M}}_{ij} = \mathbf{P}^{-1}\hat{\mathbf{R}}_{ij}\mathbf{P}^{-1}$, $\mathbf{Y} = \mathbf{P}^{-1}\mathbf{S}\mathbf{P}^{-1}$, $\overline{\mathbf{M}}_{ij} = \mathbf{P}^{-1}\overline{\mathbf{R}}_{ij}\mathbf{P}^{-1}$, $\mathbf{M} = \mathbf{R}^{-1}$ and $\mathbf{G}_j = \mathbf{N}_j\mathbf{X}^{-1}$, we have,

$$\begin{bmatrix} \mathbf{X}\mathbf{A}_i^{\mathrm{T}} + \mathbf{A}_i\mathbf{X} + \hat{\mathbf{M}}_{ij} + \hat{\mathbf{M}}_{ij}^{\mathrm{T}} + \mathbf{Y} + h\overline{\mathbf{M}}_{ij} & \mathbf{B}_i\mathbf{N}_j - \hat{\mathbf{M}}_{ij} & h\mathbf{X}\mathbf{A}_i^{\mathrm{T}} \\ \mathbf{N}_j^{\mathrm{T}}\mathbf{B}_i^{\mathrm{T}} - \hat{\mathbf{M}}_{ij}^{\mathrm{T}} & -\mathbf{Y} & h\mathbf{N}_j^{\mathrm{T}}\mathbf{B}_i^{\mathrm{T}} \\ h\mathbf{A}_i\mathbf{X} & h\mathbf{B}_i\mathbf{N}_j & -h\mathbf{M} \end{bmatrix} < 0 \quad (25)$$

From (15), it is required that $\begin{bmatrix} \overline{\mathbf{R}}_{ij} & \hat{\mathbf{R}}_{ij} \\ \hat{\mathbf{R}}_{ij}^{\mathrm{T}} & \mathbf{R} \end{bmatrix} \ge 0$. Pre-multiply and post-multiply $\mathrm{diag}\{\mathbf{P}^{-1}, \mathbf{P}^{-1}\}$ to $\begin{bmatrix} \overline{\mathbf{R}}_{ij} & \hat{\mathbf{R}}_{ij} \\ \hat{\mathbf{R}}_{ij}^{\mathrm{T}} & \mathbf{R} \end{bmatrix} \ge 0$, we have,

$$\Rightarrow \begin{bmatrix} \mathbf{P}^{-1}\overline{\mathbf{R}}_{ij}\mathbf{P}^{-1} & \mathbf{P}^{-1}\hat{\mathbf{R}}_{ij}\mathbf{P}^{-1} \\ \mathbf{P}^{-1}\hat{\mathbf{R}}_{ij}^{\mathrm{T}}\mathbf{P}^{-1} & \mathbf{P}^{-1}\mathbf{R}\mathbf{P}^{-1} \end{bmatrix} \ge 0 \Rightarrow \begin{bmatrix} \overline{\mathbf{M}}_{ij} & \hat{\mathbf{M}}_{ij} \\ \hat{\mathbf{M}}_{ij}^{\mathrm{T}} & \mathbf{X}\mathbf{M}^{-1}\mathbf{X} \end{bmatrix} \ge 0 \quad (26)$$

It should be noted that (26) is not an LMI. Based on the following property, (26) can be represented as an LMI. Consider the following inequality,

$$(\mathbf{X} - \mathbf{M})^{\mathrm{T}}\mathbf{M}^{-1}(\mathbf{X} - \mathbf{M}) = \mathbf{X}^{\mathrm{T}}\mathbf{M}^{-1}\mathbf{X} - \mathbf{X}^{\mathrm{T}} - \mathbf{X} + \mathbf{M} > 0$$

$$\Rightarrow \mathbf{X}\mathbf{M}^{-1}\mathbf{X} > 2\mathbf{X} - \mathbf{M} \quad (27)$$

From (26) and (27), it can be seen that $\begin{bmatrix} \overline{\mathbf{M}}_{ij} & \hat{\mathbf{M}}_{ij} \\ \hat{\mathbf{M}}_{ij}^{\mathrm{T}} & \mathbf{X}\mathbf{M}^{-1}\mathbf{X} \end{bmatrix} \ge \begin{bmatrix} \overline{\mathbf{M}}_{ij} & \hat{\mathbf{M}}_{ij} \\ \hat{\mathbf{M}}_{ij}^{\mathrm{T}} & 2\mathbf{X} - \mathbf{M} \end{bmatrix}$. Hence, $\begin{bmatrix} \overline{\mathbf{M}}_{ij} & \hat{\mathbf{M}}_{ij} \\ \hat{\mathbf{M}}_{ij}^{\mathrm{T}} & 2\mathbf{X} - \mathbf{M} \end{bmatrix} \ge 0$ implies $\begin{bmatrix} \overline{\mathbf{M}}_{ij} & \hat{\mathbf{M}}_{ij} \\ \hat{\mathbf{M}}_{ij}^{\mathrm{T}} & \mathbf{X}\mathbf{M}^{-1}\mathbf{X} \end{bmatrix} \ge 0$.

The stability conditions in terms of linear matrix inequalities (LMIs) [12], the connections weights of the TLFCFFNN and the maximum sampling period can be determined by solving the generalized eigenvalue minimization problem (GEVP) as stated in the following theorem.

Theorem 1: The sampled-data TLFCFFNN-based control system of (10) *formed by the continuous-time nonlinear system in form of* (2) *and the sampled-data TLFCFFNN-based controller of* (6) *is guaranteed to be asymptotically stable if there exist symmetric matrices* $\mathbf{X} \in \Re^{n\times n}$, $\mathbf{Y} \in \Re^{n\times n}$, $\overline{\mathbf{M}}_{ij} \in \Re^{n\times n}$, $\hat{\mathbf{M}}_{ij} \in \Re^{n\times n}$, $\mathbf{M} \in \Re^{n\times n}$ *and an arbitrary matrix* $\mathbf{N}_j \in \Re^{m\times n}$, $i = 1, 2, \ldots p$; $j = 1, 2, \ldots, n_h$, *such that the following LMIs hold.*

$$\mathbf{X} > 0, \mathbf{Y} > 0, \overline{\mathbf{M}}_{ij} > 0, \mathbf{M} > 0, \begin{bmatrix} \overline{\mathbf{M}}_{ij} & \hat{\mathbf{M}}_{ij} \\ \hat{\mathbf{M}}_{ij}^{\mathrm{T}} & 2\mathbf{X} - \mathbf{M} \end{bmatrix} \ge 0,$$

$$\begin{bmatrix} \overline{\mathbf{M}}_{ij} & 0 & \mathbf{X}\mathbf{A}_i^{\mathrm{T}} \\ 0 & 0 & \mathbf{N}_j^{\mathrm{T}}\mathbf{B}_i^{\mathrm{T}} \\ \mathbf{A}_i\mathbf{X} & \mathbf{B}_i\mathbf{N}_j & -\mathbf{M} \end{bmatrix} < -\frac{1}{h}\begin{bmatrix} \mathbf{X}\mathbf{A}_i^{\mathrm{T}} + \mathbf{A}_i\mathbf{X} + \hat{\mathbf{M}}_{ij} + \hat{\mathbf{M}}_{ij}^{\mathrm{T}} + \mathbf{Y} & \mathbf{B}_i\mathbf{N}_j - \hat{\mathbf{M}}_{ij} & 0 \\ \mathbf{N}_j^{\mathrm{T}}\mathbf{B}_i^{\mathrm{T}} - \hat{\mathbf{M}}_{ij}^{\mathrm{T}} & -\mathbf{Y} & 0 \\ 0 & 0 & 0 \end{bmatrix}$$

where the connection weights of the TLFCFFNN are defined as $\mathbf{G}_j = \mathbf{N}_j\mathbf{X}^{-1}$. *The maximum sampling period* h *is obtained by* $\underset{\mathbf{X},\mathbf{Y},\overline{\mathbf{M}}_{ij},\hat{\mathbf{M}}_{ij},\mathbf{M},\mathbf{N}_j}{\text{minimizing}} \frac{1}{h}$ *subject to the above LMIs.*

B. Tuning of $m_{j,i}$ and b_j

In Theorem 1, the maximum sampling period and the connection weight $g_{k,j}$ are determined based on the LMI approach. In this section, the connection weight $m_{j,i}$ and the bias b_j will be determined. Owning to the nonlinear nature of the activation function of the TLFCFFNN, it is difficult to formulate the finding of $m_{j,i}$ and b_j into an LMI problem. Instead, GA can be employed to tune the values of $m_{j,i}$ and b_j by minimizing the following performance index,

$$J = \int_0^{t_1} \begin{bmatrix} \mathbf{x}(t) \\ \mathbf{u}(t) \end{bmatrix}^{\mathrm{T}} \begin{bmatrix} \mathbf{J}_1 & \mathbf{J}_2 \\ \mathbf{J}_2^{\mathrm{T}} & \mathbf{J}_3 \end{bmatrix} \begin{bmatrix} \mathbf{x}(t) \\ \mathbf{u}(t) \end{bmatrix} dt \quad (28)$$

It should be noted that the values of the sampling period h and the connection weight $g_{k,j}$ are kept constant during the turning process. As the system stability is determined by the sampling period and the connection weight $g_{k,j}$ only, the values of $m_{j,i}$ and b_j can be freely tuned to optimize the system performance. During the tuning process, $m_{j,i}$ is the gene to form the chromosome of the GA process.

C. Design Procedure

The design procedure of the sampled-data TLFCFFNN-based controller is given as follows.

Step I) Obtain the model of the nonlinear plant in the form of (2).

Step II) Determine the number of hidden node n_h and the activation functions for the sampled-data TLFCFFNN-based controller in the form of (6).

Step III) Determine the maximum sampling period, $h_{\max}$, and the connection weight $g_{k,j}$ by Theorem 1. Choose a constant sampling period $0 \le h \le h_{\max}$.

Step IV) Under the chosen sampling period h and the connection weight $g_{k,j}$, obtain the connection weight $m_{j,i}$ and the bias b_j by the GA process. Realize the sampled-data TLFCFFNN-based controller based on the determined h, $g_{k,j}$, $m_{j,i}$ and b_j.

IV Application Example

The proposed sampled-data TLFCFFNN-based controller will be employed to stabilize an inverted pendulum subject to parameter uncertainties. The objective is to drive all the system states of the inverted pendulum to zero at the steady state.

Step I) The system behaviour of the inverted pendulum is described by the following dynamic equation.

$$\ddot{\theta}(t)=\frac{g\sin(\theta(t))-am_pL\dot{\theta}(t)^2\sin(2\theta(t))/2-a\cos(\theta(t))u(t)}{4L/3-am_pL\cos^2(\theta(t))} \tag{29}$$

where $\theta(t)$ is the angular displacement of the pendulum, g = 9.8m/s^2 is the acceleration due to gravity, $m_p \in [m_{p_{\min}} \quad m_{p_{\max}}]$ = [2 5]kg is the mass of the pendulum, $M_c \in [M_{c_{\min}} \quad M_{c_{\max}}]$ = [30 35]kg is the mass of the cart, $a = 1/(m_p + M_c)$, $2L$ = 1m is the length of the pendulum, and $u(t)$ is the force applied to the cart. m_p and M_c contain parameter uncertainties of the system. The inverted pendulum subject to parameter uncertainties can be represented by the following model,

$$\dot{\mathbf{x}}(t)=\sum_{i=1}^{4}w_i\left(\mathbf{A}_i\mathbf{x}(t)+\mathbf{B}_iu(t)\right) \tag{30}$$

where $\mathbf{x}(t)=[x_1(t) \quad x_2(t)]^{\mathrm{T}}=[\theta(t) \quad \dot{\theta}(t)]^{\mathrm{T}}$,

$x_1(t)\in[x_{1_{\min}} \quad x_{1_{\max}}] = \left[-\frac{\pi}{3} \quad \frac{\pi}{3}\right]$ and $x_2(t)\in[x_{2_{\min}} \quad x_{2_{\max}}]$ = [−5 5]; $f_1(\mathbf{x}(t))=\frac{g-am_pLx_2(t)^2\cos(x_1(t))}{4L/3-am_pL\cos^2(x_1(t))}\left(\frac{\sin(x_1(t))}{x_1(t)}\right)$ and $f_2(\mathbf{x}(t))=-\frac{a\cos(x_1(t))}{4L/3-am_pL\cos^2(x_1(t))}$;

$\mathbf{A}_1=\mathbf{A}_2=\begin{bmatrix}0 & 1\\ f_{1_{\min}} & 0\end{bmatrix}$ and $\mathbf{A}_3=\mathbf{A}_4=\begin{bmatrix}0 & 1\\ f_{1_{\max}} & 0\end{bmatrix}$;

$\mathbf{B}_1=\mathbf{B}_3=\begin{bmatrix}0\\ f_{2_{\min}}\end{bmatrix}$ and $\mathbf{B}_2=\mathbf{B}_4=\begin{bmatrix}0\\ f_{2_{\max}}\end{bmatrix}$; $f_{1_{\min}}$ = 11.3533 and $f_{1_{\max}}$ = 16.4640, $f_{2_{\min}}$ = −0.0192 and $f_{2_{\max}}$ = −0.0492;

$w_i(\mathbf{x}(t))=\frac{\mu_{\mathrm{M}_1^i}(f_1(\mathbf{x}(t)))\times\mu_{\mathrm{M}_2^i}(f_2(\mathbf{x}(t)))}{\sum_{l=1}^{4}\left(\mu_{\mathrm{M}_1^l}(f_1(\mathbf{x}(t)))\times\mu_{\mathrm{M}_2^l}(f_2(\mathbf{x}(t)))\right)}$;

$\mu_{\mathrm{M}_1^\beta}(f_1(\mathbf{x}(t)))=\frac{-f_1(\mathbf{x}(t))+f_{1_{\max}}}{f_{1_{\max}}-f_{1_{\min}}}$ for β = 1, 2;

$\mu_{\mathrm{M}_1^\delta}(f_1(\mathbf{x}(t)))=1-\mu_{\mathrm{M}_1^l}(f_1(\mathbf{x}(t)))$ for δ = 3, 4;

$\mu_{\mathrm{M}_2^\kappa}(f_2(\mathbf{x}(t)))=\frac{-f_2(\mathbf{x}(t))+f_{2_{\max}}}{f_{2_{\max}}-f_{2_{\min}}}$ for κ = 1, 3 and

$\mu_{\mathrm{M}_2^\phi}(f_2(\mathbf{x}(t)))=1-\mu_{\mathrm{M}_2^l}(f_2(\mathbf{x}(t)))$ for ϕ = 2, 4.

Step II) A sampled-data TLFCFFNN-based controller with four hidden nodes is employed to handle the inverted pendulum. From (6), the sampled-data TLFCFFNN-based controller is given by,

$$u(t)=\sum_{j=1}^{4}m_j(\mathbf{x}(t_\gamma))\mathbf{G}_j\mathbf{x}(t_\gamma),\ t_\gamma\le t<t_{\gamma+1}$$

where the logarithmic sigmoid function is employed as the transfer function, i.e, $t_f\left(\sum_{i=1}^{n}m_{j,i}x_i(t_\gamma)+b_j\right)=\frac{1}{1+e^{-\left(\sum_{i=1}^{n}m_{j,i}x_i(t_\gamma)+b_j\right)}}$.

Step III) The maximum sampling period, $h_{\max}$, is found to be 0.0284s based on Theorem 1. A constant sampling period $0 < h = 0.02 < h_{\max}$ is chosen for the sampled-data TLFCFFNN-based controller. MATALB LMI tool box is employed to solve the solution of the GEVP in Theorem 1 numerically. The connection weights, $\mathbf{G}_j=\mathbf{N}_j\mathbf{X}^{-1}$, are obtained as $G_1 = [g_{1,1} \quad g_{2,1}]$ = [1358.9268 347.8515], $G_2 = [g_{1,2} \quad g_{2,2}] = G_3 = [g_{1,3} \quad g_{2,3}]$ = [1319.7667 337.4474] and $G_4 = [g_{1,4} \quad g_{2,4}]$ = [1291.0126 329.7995]. It can be concluded from Theorem 1 that the optimized sampled-data TLFCFFNN-based control system is asymptotically stable.

Step IV) The parameters $m_{j,i}$ and b_j of the activation function $t_f\left(\sum_{i=1}^{2}m_{j,i}x_i(t_\gamma)+b_j\right)=\frac{1}{1+e^{-\left(\sum_{i=1}^{2}m_{j,i}x_i(t_\gamma)+b_j\right)}}$ can be obtained by optimizing the following performance index using improved GA [16] under m_c = 2kg and M_p = 30kg.

$$J=\int_0^{t_\gamma}\begin{bmatrix}\mathbf{x}(t)\\ u(t)\end{bmatrix}^{\mathrm{T}}\begin{bmatrix}\mathbf{J}_1 & \mathbf{J}_2\\ \mathbf{J}_2^{\mathrm{T}} & \mathbf{J}_3\end{bmatrix}\begin{bmatrix}\mathbf{x}(t)\\ u(t)\end{bmatrix}dt_\gamma \tag{31}$$

The values of the connection weight and bias, $m_{j,i}$ and b_j, before and after GA process are listed in Table I. The obtained sampled-data TLFCFFNN-based controller is employed to handle the inverted pendulum subject to parameter uncertainties. Under the initial state conditions of $\mathbf{x}(0)=\begin{bmatrix}\frac{\pi}{3} & 0\end{bmatrix}^{\mathrm{T}}$ $\mathbf{x}(0)=\begin{bmatrix}\frac{\pi}{6} & 0\end{bmatrix}^{\mathrm{T}}$, $\mathbf{x}(0)=\begin{bmatrix}-\frac{\pi}{6} & 0\end{bmatrix}^{\mathrm{T}}$ and $\mathbf{x}(0)=\begin{bmatrix}-\frac{\pi}{3} & 0\end{bmatrix}^{\mathrm{T}}$ with m_c = 2kg and M_p = 30kg, the system responses and control signals of the sampled-data TLFCFFNN-based control systems are shown in Fig. 2. Referring to these figures, it can be seen that the proposed sampled-data TLFCFFNN-based controller is able to stabilize the inverted pendulum. The proposed sampled-data TLFCFFNN-based controller can be easily implemented by a microcontroller or a digital computer.

V. Conclusion

A sampled-data TLFCFFNN-based controller, which is formed by a sampler, a TLFCFFNN and a ZOH unit, has been proposed for continuous-time nonlinear systems. Based on the Lyapunov-based approach, the stability of the sampled-data TLFCFFNN-based control systems has been investigated. Stability conditions have been derived to guarantee the stability of the sampled-data TLFCFFNN-

based control systems respectively. The findings of the maximum sampling period and the network connection weights, and the optimization of system performance have been formulated as generalized eigenvalue and genetic algorithm minimization problems. An application example on stabilizing an inverted pendulum subject to parameter uncertainties has been given to illustrate the design procedure and the effectiveness of the proposed approach.

REFERENCES

[1] B. Widrow and M.A. Lehr, "30 years of adaptive neural networks: Perceptron, madaline, and backpropagation," *Proceedings of the IEEE*, vol. 78, no. 9, Sept. 1990, pp. 1415-1442.

[2] G.P. Liu, V. Kadirkamanathan, and S.A. Billings, "Variable neural networks for adaptive control of nonlinear systems," *IEEE Transactions on System, Man, and Cybernetic – Part C: Applications and Reviews*, vol. 29, no.1, pp. 34-43, Feb. 1999.

[3] H.D. Patiño, R. Carelli, and B.R. Kuchen, "Neural network for advanced control of robot manipulators," *IEEE Transactions on Neural Networks*, vol. 13, no.2, pp. 343-354, March 2002.

[4] R.M. Sanner and J.J.E. Slotine, "Gaussian networks for direct adaptive control," *IEEE Transactions on Neural Networks*, vol. 3, no. 6, pp. 837-863, Nov. 1992.

[5] R. Carelli, E.F. Camacho and D. Patiño, "A neural network based feedforward adaptive controller for robots," *IEEE Transactions on Systems, Man, and Cybernetics*, vol. 25, no. 9, pp. 1281-1288, Sept. 1995.

[6] C.L. Hwang, "Neural-network-based variable structure control of electrohydralic servosystems subject to huge uncertainties without persistent excitation," *IEEE Transactions on Mechatronics*, vol. 4, no. 1, pp. 50-59, March 1999.

[7] S. Lin and A.A. Goldenberg, "Neural-network control of mobile manipulators," *IEEE Transactions on Neural Networks*, vol. 12, no. 5, pp. 1121-1133, Sept. 2001.

[8] C.L. Lin, "Control of perturbed systems using neural networks," *IEEE Transactions on Neural Networks*, vol. 9, no. 5, pp. 1046-1050, Sept. 1998.

[9] K. Tanaka, "Stability and stabilizability of fuzzy-neural-linear control systems," *IEEE Transactions on Fuzzy Systems*, vol. 3, no. 4, pp. 438-447, Nov. 1995.

[10] K. Tanaka, "An approach to stability criteria of neural-network control systems," *IEEE Transactions on Neural Network*, vol. 7, no. 3, pp. 629-642, May 1996.

[11] J.D. Hwang and F.H. Hsiao, "Stability analysis of neural network interconnected systems," *IEEE Transactions on Neural Networks*, vol. 14, no. 1, pp. 201-208, Jan. 2003.

[12] S. Boyd, L. El. Ghaoui, E. Feron, and V. Balakrishnan, *Linear matrix inequalities in system and control theory*. SIAM, Philadelphia, 1994.

[13] Z. Michalewicz, *Genetic Algorithm + Data Structures = Evolution Programs*, 2nd Ed. Springer-Verlag, 1994.

[14] F.M. Ham and I. Kostanic, *Principles of Neurocomputing for Science & Engineering*, McGraw Hill, 2001.

[15] B.D.O. Anderson and J.B. Moore, *Optimal Control: Linear Quadratic Methods*. Prentice Hall, 1990.

[16] F.H.F. Leung, H.K. Lam, S.H. Ling and P.K.S. Tam, "Tuning of the structure and parameters of neural network using an improved genetic algorithm," *IEEE Trans. Neural Networks*, vol. 14, no. 1, pp. 79-88, Jan. 2003.

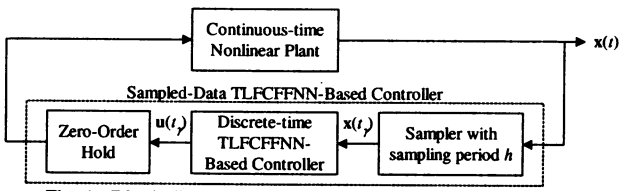

Fig. 1. Block diagram of a TLFCFFNN-based control system.

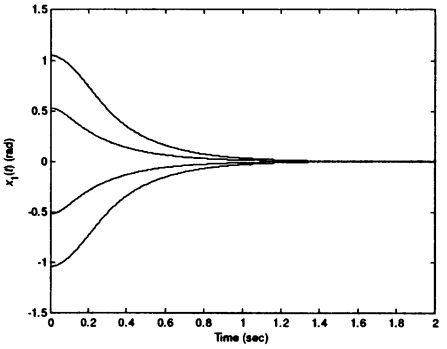

Fig. 2(a). $x_1(t)$.

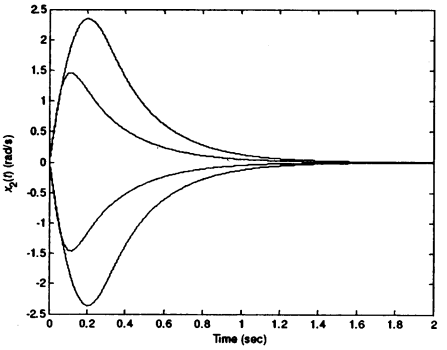

Fig. 2(b). $x_2(t)$.

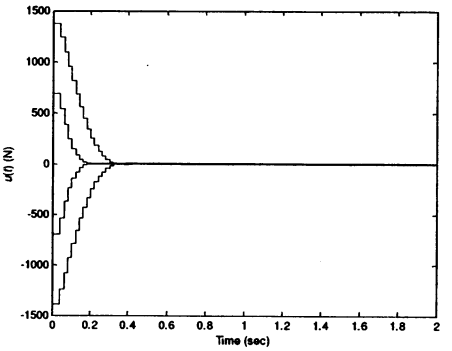

Fig. 2(c). $u(t)$

Fig. 2. System responses and control signals of the inverted pendulum with the proposed sampled-data TLFCFFNN-based controller for $m_p = 2$kg and $M_c = 30$kg.

TABLE I. THE VALUES OF THE CONNECTION WEIGHT AND BIAS, $M_{i,l}$ AND B_i, BEFORE AND AFTER THE GA PROCESS.

Parameter	Initial parameter values	Parameter values after GA process
$m_{1,1}$	–0.0591	–0.7283
$m_{1,2}$	0.5511	–0.7605
b_1	–0.2765	–0.2638
$m_{2,1}$	–0.9863	0.8534
$m_{2,2}$	0.5118	–0.8836
b_2	–0.3234	0.9208
$m_{3,1}$	0.3058	0.9816
$m_{3,2}$	0.1582	0.9656
b_3	–0.7899	0.8918
$m_{4,1}$	–0.6254	0.9972
$m_{4,2}$	–0.7569	0.9993
b_4	0.4423	0.8240